Science of the Total Environment 514 (2015) 298–306

Contents lists available at ScienceDirect

Science of the Total Environment

journal homepage: www.elsevier.com/locate/scitotenv

Photogrammetry for environmental monitoring: The use of drones and hydrological models for detection of soil contaminated by copper

Alessandra Capolupo [a], Stefania Pindozzi [a], Collins Okello [b], Nunzio Fiorentino [a], Lorenzo Boccia [a,*]

[a] University of Naples Federico II, Department of Agricultural Sciences, via Università 100, 80055 Portici Naples, NA, Italy
[b] Gulu University, Department of Biosystems Engineering, P.O. Box 166, Gulu, Uganda

HIGHLIGHTS

- Soil sampling and analysis to investigate copper concentration is very expensive.
- A method aimed to increase the effectiveness of investigation is proposed.
- The method involves photogrammetry, hydrology and wetlands prediction indices.
- High resolution DEM (30 mm) has been generated.
- Prediction indices are able to detect areas of Cu accumulation at plot scale.

ARTICLE INFO

Article history:
Received 4 November 2014
Received in revised form 30 January 2015
Accepted 30 January 2015
Available online xxxx

Editor: D. Barcelo

Keywords:
Photogrammetry
Drones
Copper soil pollution
Wetlands
Topographic Index
Clima-Topographic Index

ABSTRACT

Campania Region of Southern Italy has a complex environmental situation, due to geogenic and anthropogenic soil pollution. Some of the pollutants such as copper are mobilized in the organic matter. It has been shown that wetlands provide physical as well as biogeochemical barriers against pollutants. Therefore, the objective of this study was to introduce and test an innovative approach able to predict copper accumulation points at plot scales, using a combination of aerial photos, taken by drones, micro-rill network modelling and wetland prediction indices usually used at catchment scales. Data were collected from an area measuring 4500 m^2 in Trentola Ducenta locality of Caserta Province of southern Italy. The photos processing with a fifth generation software for photogrammetry resulted in a high resolution Digital Elevation Model (DEM), used to study micro-rill processes. The DEM was also used to test the ability of Topographic Index (TI) and the Clima-Topographic Index (CTI) to predict copper sedimentation points at plot scale (0.1–10 ha) by comparing the map of the predicted and the actual copper distribution in the field. The DEM obtained with a resolution of 30 mm showed a high potential for the study of micro-rill processes and TI and CTI indices were able to predict zones of copper accumulation at a plot scale.

1. Introduction

Currently, Campania Region, in South Italy, is facing one of the most critical environmental problems due to agricultural soil pollution by accidental contamination. Unfortunately, the overall situation is heterogeneous and complex. Between the years 1998 and 2008, six of the 55 National Interest Priority Site (NIPS) gazetted in Italy were located in Campania Region (Vito et al., 2009). Of the six NIPS, Domitian Coast Flegreo and Agro Aversano were selected as most important in Campania Region (Law no. 426 of 1998). In addition, the National Institute of Health has included these NIPS areas among the 44 Italian regions with high levels of cancer risk, due to the different and numerous pollutants found in soil such as heavy metals.

High concentrations of heavy metals in Campania Region are a result of a combination of geogenic pollution caused by natural phenomena, and anthropogenic pollution due to voluntary or accidental activities (Cicchella et al., 2005). Geogenic pollution is essentially linked to the processes of parent rock genesis that are extremely rich of metallic elements, due to volcanic activities and related events, such as hot springs and fumaroles (De Vivo et al., 1995). Anthropogenic pollution is mainly related to industrial activities, which produce high concentrations of cadmium (Cd), chromium (Cr), copper (Cu), mercury (Hg), lead (Pb), nickel (Ni), and zinc (Zn) (Filippelli et al., 2012). Motor vehicle traffic also results in high concentrations of Cd, Cr, Cu, Ni, Pb, selenium (Se) and Zn in the areas near driveways (Albanese and Cicchella, 2012). Use of inorganic pesticides and chemical fertilizers could result in soil

* Corresponding author at: University of Naples Federico II, Department of Agricultural Sciences, Via Università 100, 80055 Portici Naples, (NA), Italy.
E-mail addresses: alessandra.capolupo@unina.it (A. Capolupo), stefania.pindozzi@unina.it (S. Pindozzi), collins.okello@gmail.com (C. Okello), nunzio.fiorentino@unina.it (N. Fiorentino), lorenzo.boccia@unina.it (L. Boccia).

http://dx.doi.org/10.1016/j.scitotenv.2015.01.109
0048-9697/

pollution by Cu, Hg, manganesium (Mn), Pb and Zn (Swaine, 1962). Other causes of soil pollution include point sources like gasoline pumps and illegal dumping of household waste (Lima et al., 2012). Nowadays, the mapping of geogenic pollutants in Campania Region is known and predictable (Albanese et al., 2007). However, it is still very difficult to predict the diffusion and distribution of anthropogenic contaminants.

Among anthropogenic pollutants, the copper has a significant importance in agronomy since it is an essential element, although in high concentrations has a strong toxic effect on plants and animals. Belonging to group 11 elements of the periodic table, its electronic level is incomplete; therefore, it is a very versatile ion that can interact chemically with the organic and mineral soil components. Due to its ability, it is not very mobile in the soil and, therefore, tends to accumulate in the superficial soil layers (Kabata-Pendians and Pendias, 2001). Mobility of copper in soil is essentially related to chelation by organic matter and adsorption processes, which is highly dependent on the pH of the soil. It has been demonstrated that 1 g of humic acids has the ability to chelate from 48 to 60 mg of copper (Stevenson and Ficht, 1981). For this reason, copper accumulates in the superficial soil layers.

Because their diffusion is "patchy", it is really difficult to predict the extent and the location of pollutants. Current methods for determining distribution of pollutants require carrying out a characterization procedure involving analysis of a large set of organic and inorganic substances in each unit of homogeneous soil. These procedures are rather laborious and expensive. Typically, the characterization is carried on a grid of 10×10 m, resulting in 100 samples per ha. It is therefore extremely difficult and expensive to sample and characterize soil from the entire region with a sufficiently dense mesh. Another technique involves the use of imaging spectroscopy. It is utilized to identify spatial mineral patterns and to monitor temporal changes in contaminated river sediments (Buzzi et al., 2014).

Some landscape structures can be considered as physical or biogeochemical barriers against contaminants, when they are set between the source of polluted water and the receiving water body (Muscutt et al., 1993). Wetlands play a fundamental role, due to their structural characteristics, they are classified as area buffers. Wetlands fulfil this role through absorption of the pollutants by plants and dilution in the absence of significant nitrogen concentration and by denitrification processes (Montreuil, 2011). Infascelli et al. (2013) tested the efficiency of different topographical and hydrological indices suited to predict wetland distribution at the catchment scale. It is likely that similar approaches may be transferred to plot scales (Capolupo et al., 2014).

In particular, Topographic Index (TI) has widely been used for estimating the spatial distribution of soil moisture and runoff source areas (Chirico et al., 2003). In particular, it has been applied for studying spatial scale effects on hydrological processes (Sivapalan and Wood, 1987; Beven et al., 1988; Sivapalan et al., 1990; Famiglietti and Wood, 1991), for identifying flow paths (Robson et al., 1992), for characterizing biological processes (White and running, 1994), vegetation patterns (Moore et al., 1993) and forest site quality (Holmgren, 1994) and for predicting wetland distribution (Merot et al., 2003). This index is usually calculated from elevation data (Sörensen et al., 2006). Indeed, the digital terrain analysis produces an intermediate dataset that includes the spatial discretization of the terrain in elemental units, the connectivity among these elements and, terrain attributes (Chirico et al., 2005). Results of digital terrain analysis must be used in consequently terrain-based hydrological application (Chirico et al., 2005).

At plot scales, the calculation of the indices to describe the spatial distribution of soil moisture must be based on an extremely accurate and precise Digital Elevation Model (DEM) (Chirico et al., 2005). Several devices can be used to generate high precision DEM. A common example involves use of laser scanners (Khorashahi et al., 1987; Huang et al., 1988; Bertuzzi et al., 1990; Romenkens et al., 1986). It allows for improved resolution and accuracy of the resulting DEM, though it requires considerable amount of time for data collection and processing. However, Rieke-Zapp et al. (2001) proposed photogrammetric techniques to generate DEM. The accuracy and the resolution of DEM produced by photogrammetric techniques were similar to those obtained with the laser scanner, while time required for data collection reduced significantly.

The introduction of important innovations such as drones and fifth generation software for photogrammetry may significantly improve the results. Drones could allow for reduced flight quotas and to reach difficult-to-access areas; therefore, resulting in a drastic decrease in the time and costs of data acquisition and of the entire operation of monitoring (Nex and Remondino, 2014). It also makes it possible to obtain high resolution aerial photos at plot scale. The fifth generation software can process hundreds of digital images at the same time and to obtain their automatic restitution leading to a significant reduction in photo/image processing time (Pierrot-Deseilligny et al., 2011).

Natural phenomena characteristics vary considerably in space and time (West and Shlesinger, 1990), because of many interacting factors, some of which operate over large distances, other over long time periods. This variability contains both trend and random factors. Random component is a structural, scale-dependent element, for which, at least within a specific radius of influence, the spatial differences between the properties of the soil can be expressed, rather than in absolute terms, as a function of the distance of separation between the sampling points (Castrignanò and Stelluti, 1997). It follows, then, that temporal and spatial variability is strongly influenced by scale and variables of observation. Therefore, it is necessary to define the methods suited to estimate the values of the natural phenomenon properties being studied, where measured data are not available. So, no deterministic model can describe spatial variability because it is based on the application of an algorithm defined a priori (Castrignanò et al., 2011). On the contrary, statistical models can assess and model spatial variation (Castrignanò et al., 2011). In particular, spatial relationships among data values can be quantified and processed by the modern statistical theory, based on the theory of regionalized variables (geostatistics) (Journel and Huijbregts, 1978; Goovaerts, 1987).

Areas with accumulated copper such as wetlands have been compared to sedimentation micro-basins. In the present study, the possibility of predicting the distribution of copper sedimentation/accumulation points at plot scale was explored. It is important to underline that the terms "accumulation" and "sedimentation" are used interchangeably to indicate the copper storage at a point, following a micro-runoff process. The method employed, considers different approaches, used in other context to determinate the distribution of wetlands at catchment scale. It involves application of drones, fifth generation software for photogrammetry, modelling of transport processes and geostatistics.

2. Study area

The study area is located in the municipality of Trentola Ducenta, in Caserta Province. It is at an altitude of 68 m above mean sea level and is one of 77 municipalities of the NIPS Litorale Domizio Flegreo and Agro Aversano. The experiment was conducted in an area measuring 4500 m^2 (Fig. 1), suspected of being contaminated with heavy metals and organic pollutants. Soil samples were taken from the site at regular mesh of 5×5 m, for a total of 170 points. For each point, the concentration of 15 elements was carried on all samples found to have traces of pollutants.

Analyses of soil samples were conducted by the Mass Spectrometry Laboratory of University of Naples Federico II, by applying the method EPA 6010C 2007. Each sample have been first reacted with nitric acid and has been made up to a final volume in a volumetric flask with a reagent water, and, then, analyzed by inductively coupled plasma-atomic emission spectrometry (ICP-AES), that measures characteristic emission spectra using an optical spectrometry. Indeed, aerosol, resulting from a nebulisation process of the samples, is transported to the plasma torch, where a radio-frequency inductively coupled plasma produces a

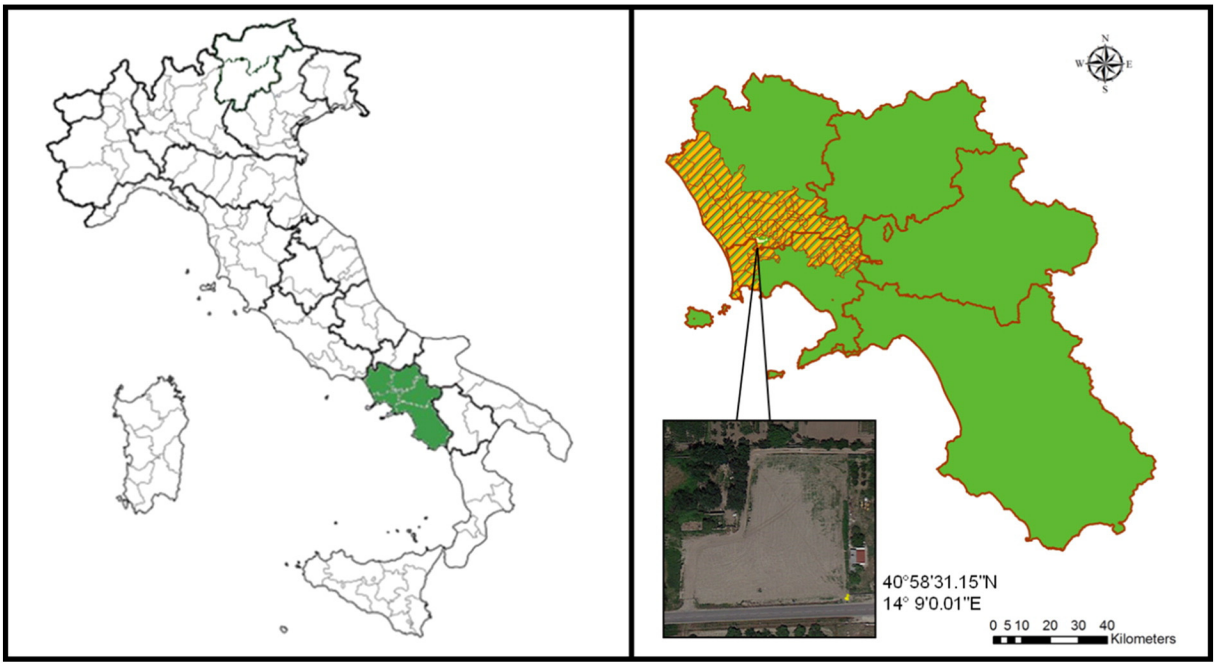

Fig. 1. Study area.

specific emission. Photosensitive devices monitor intensities of the emission.

3. Material and methods

3.1. Prediction of the accumulation area distribution

For the purpose of the research, the accumulation areas were assimilated to sedimentation zones, similarly to wetlands. Over the years, several indices were proposed to predict wetland distribution. Beven and Kirkby (1979) proposed a Soil Topographic Index (STI) given by Eq. (1).

$$STI = \ln\left(\frac{\alpha}{T\tan\beta}\right) \quad (1)$$

where, α is the drainage area, β is the local slope and T is the trasmissivity. However, it has been observed that in most cases, the transmissivity can be neglected compared to the value of the area of drainage and that of the variation of the local slope (O'loughlin, 1981; Oosterbaan and Nijland, 1994; Lagacherie et al., 2006). Therefore, Beven and Kirkby (1979) and Beven (1986) proposed the Topographic Index (TI) given by Eq. (2).

$$TI = \ln\left(\frac{\alpha}{\tan\beta}\right) \quad (2)$$

For a certain rainfall depth, the larger the drainage basin and the smaller the slope, the higher TI value will be. So, a more robust index for predicting wetland distribution, called the Clima-Topographic Index (CTI) given by Eq. (3), was introduced (Merot et al., 2003).

$$CTI = \ln\left(\frac{Vr}{\tan\beta}\right) \quad (3)$$

In addition to the topographical aspects, it considers the volume of effective annual rainfall *Vr*, computed by multiplying drainage area with the mean annual effective rainfall depth. The mean annual effective rainfall is determined using Eq. (4) (Merot et al., 2003).

$$Reff_{annual} = \sum_{1-12} Reff_i \quad (4)$$

where, Re ff_i is the monthly effective rainfall depth, obtained from the difference between the rainfall depth (R_i) and the potential evapotranspiration (PET_i).

$$Reff_i = R_i - PET_i \quad (5)$$

when,

$$R_i \le PET_i \quad Reff_i = 0.$$

This study used the Hargreaves Equation (Hargreaves et al., 1985). Hargreaves Equation (Eq. (6)) is preferred to other evapotranspiration equation as it requires only temperature data and it is easily calculated (Pindozzi et al., 2012, 2013). Moreover, it is suitable to estimate annual evapotranspiration at the local climate condition in the study area (Pindozzi et al., 2012, 2013).

$$PET_i = 0.0023 \times R_a \times (T_{mean} + 17.8) \times \sqrt{(T_{max} - T_{min})} \quad (6)$$

1) evapotranspiration (ET_o)
2) potential evapotranspiration (PET_i)

where, PET_i (ET_o) is the potential evapotranspiration in mm day^{-1}, R_a is the extraterrestrial radiation in MJ m^{-2} day^{-1}; T_{mean}, T_{max} and T_{min} are the mean, maximum and minimum daily temperature in °C, respectively. R_a was calculated by using methods reported in Allen et al. (1998).

In the calculation of the CTI, the local slope was replaced with the downhill slope, defined as the slope between the point of interest and the course of runoff, measured along the flow direction. It was

shown that this substitution improves the results, both from the technical (the local slope is smoothed with the downhill slope) and conceptual points of views (soil saturation depends not only on the upslope factor but also on the down-slope factors, not considered with TI) (Gascuel-Odoux et al., 1998). Merot et al. (2003) showed that this index was able to determine the location and general area extent of wetlands in a reliable manner without calibration in most cases. It fails only when the soils are characterized by high heterogeneous permeability. The field examined in this study did not have these features.

3.2. Geostatistics background

Geostatistics allow to predict the spatial distribution of a variable property thanks to kriging interpolation. The basic form of kriging is simple kriging, in which the unknown value z ($\boldsymbol{x}_0$) (value to be estimated) of a given realization of $Z(\boldsymbol{x_0})$ is predicted from a linear combination of the observations (known values close to a point to be estimated $z(\boldsymbol{x_i})$ $i = 1, 2, \ldots, N$, at the support points $\mathbf{x_i}$), given by Eq. (7):

$$z^*_{SK}(\mathbf{x}_0) = \sum_{i=1}^{N} \lambda_i z(\mathbf{x}_i) + \left[1 - \sum_{i=1}^{N} \lambda_i\right] m \tag{7}$$

where λ_i are weights and m is a known constant mean of the area of interest.

A more complex form is represented by Indicator Kriging (Journel, 1983). This approach is particularly suitable for the treatment of environmental data, because, being a non-parametric method (no prior assumption about the shape or type of the conditional distribution), it allows to estimate the probability of exceeding an attribute under investigation of a threshold value (Castrignanò et al., 2000). Indeed, the attribute value is assigned 0 if it is below the threshold value or 1 if it is above the threshold value (Tavares et al., 2008).

Kriging is a very useful interpolator thanks to the following properties (Castrignanò et al., 2011):

- the obtained value is as accurate as possible from the data available;
- given that error term is calculated together with the estimation, the kriged value can be used with a degree of confidence;
- It is an exact interpolator (the estimated values are identical to the observed values when an interpolated location coincides with a sample location).

Fig. 2. The drone Tarot FY690s equipped with all hardware components and software tools.

3.3. Generation of the digital elevation model

The essential baseline information for the morphometric analysis of the soil and extraction of micro-rill network is the Digital Elevation Model (DEM). To obtain a high resolution DEM, the entire study area was surveyed using a prototype drone, Tarot FY690s shown in Fig. 2.

The drone was equipped with all necessary hardware components and software tools, required for its control and programming, and with the basic software for planning of the flight. The drone was mounted with a Canon PowerShot S100 camera of 12.1 Megapixels, 7.44 × 5.58 mm sensor and 5.2 mm focal length. This camera was calibrated using the Agisoft Lens software.

In order to get a ground sample distance (GSD) of 10 mm and in consideration of a safety factor of 10%, the flight altitude has been set at 25 m. Ten (10) targets with appropriate support were placed along the perimeter of the field and in its central zone. The locations of the targets were determined using a total station Geodimeter 600 with angular accuracy of 3″ (10 cm^3), i.e., 1.0 mgon, and distance measurement accuracy of ±(5 mm + 3 ppm). A precision of 1.7 mm in height difference (sen 0.010 ∗ 100) at a distance of 100 m and a precision equal to 5 mm in planimetric is expected. These points have been used as ground control points (GCP) for post-processing purposes (Nex and Remondino, 2014). The topographic reconstruction of the detailed survey has been carried out using the Meridiana software.

Aerial photo orientation and georeferencing were the preliminary steps of metric reconstruction of the scene. As suggested by Triggs et al. (2000) and Gruen and Beyer (2001), imagery orientation consists photo alignment and tie point extraction. Moreover, in order to improve image orientation, minimize photo block deformation and to georeference the imagery, GCPs have been imported in the alignment. At the end of this process, a polygonal model (mesh) has been generated and elaborated to obtain texture mapping, orthophoto and DEM. Processing of the photos has been made by applying Agisoft PhotoScan Professional software.

Major information about the methodological approach (drone choice, planning of the flights, camera calibration, photos processing are reported in previous work (Capolupo et al., 2014)).

3.4. Micro-rill network and copper sedimentation points

The DEM has been converted to GRID format using ESRI ArcGIS 10.0 Software by interpolating the original points with the Kriging estimator. The obtained model is more suitable for processing due to its regular structure. Subsequently, the identification and the filling of the "pits" has been made with ArcGIS' Hydrology tool, that removes small imperfections in the data. The pits are raster cells without outlets that create discontinuities in the micro-rill network and possible abnormality drainage (Infascelli et al., 2013). The surface flow direction has been drawn using the eight flow direction (D8) model, also called monodirectional model (O' Callaghan and Mark, 1984). It has been shown that D8 models are particularly suitable for the modelling of the hydro-graphic network (Wolock and McCabe, 1995; Beaujouan et al., 2001).

Micro-basins were found out by applying outlets. For each of them, the essential parameters for the calculation of the TI and the CTI were estimated. Information on the effective and mean annual rainfall, temperature and evapotranspiration is required for evaluating the CTI of the study area over the area basin and slope. Therefore, the precipitation records from two neighbouring meteorological stations located at S.A. Pizzone and Caiazzo, were analyzed and used to compute the two indices. These data are daily official data published in "Annali Idrologici e altre pub. Del compartimento di Napoli del S.I.M.N.". They relate to a period of about 20 years, from 1977 to 1993.

To validate the model and choose the best strategies to predict the copper sedimentation points, results were interpolated with simple

kriging using ArcGis' Geostatistical Analyst tool and compared with the actual mapping of the copper on the soil surface.

Moreover, in order to verify the relationship between copper concentration and TI (or CTI), the Boolean Operation between layer of TI (or CTI) and copper concentration, interpolated with Indicator Kriging, was achieved. In particular, the Indicator Kriging interpolation was obtained by applying ArcGis' Geostatistical Analyst tool. The threshold value for the Indicator Kriging was defined according to the Italian legal limit of copper concentration (T.U. Ambientale 156/06). The "Boolean And" Operation was implemented thanks to the application of ArcGis' Spatial Analyst tool. This function multiplies the cell values of the two input raster, so that it, if both input values are true (equal 1), the output value is 1; otherwise, the output value is 0. The true values for the interpolated copper concentration correspond to the highest values of copper concentration (greater than the Italian legal limit of 120 mg kg^{-1}), instead, for the TI (or CTI) correspond to maximum value of TI (or CTI).

4. Results

4.1. Spatial distribution of Cu contents in soil samples

Traces of Cu were detected overall the study area although, in varying concentrations. Concentrations were found to be greater than the Italian legal limit of 120 mg kg^{-1} (T.U. Ambientale 156/06) in 7 different hotspots, as shown in Fig. 3. However, other points of the area of interest exhibit border line concentrations of Cu as illustrated in Fig. 3.

The copper concentration map, interpolated with Indicator Kriging, is shown in Fig. 4.

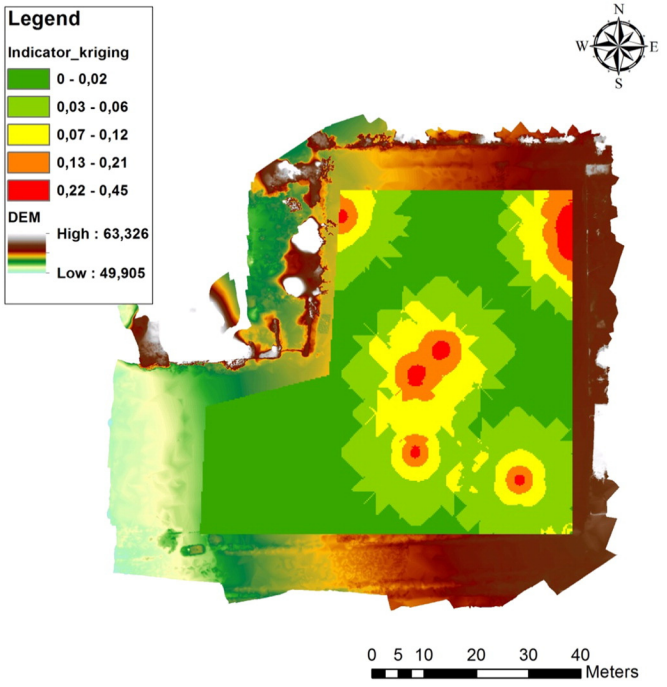

Fig. 4. Map of copper concentration interpolated with Indicator Kriging.

4.2. Survey area reconstruction

During data collection, the drone has been flown at a height of 25 m and speed of 4 m s^{-1}. This resulted in longitudinal and transversal overlap strips 70% and 30%, respectively. The coverage of the entire area has been achieved by acquisition of 42 frames, though a total of 84 pictures were taken, since a pair of shots were taken at each of the waypoint identified. This has been achieved during three different flight missions. The first two missions were each characterized by 16 waypoints, over a period of 12 min and the third had 12 waypoints and lasted for 8 min.

The blocks of images allowed for the generation of a very detailed orthophoto and a very high resolution DEM. Actually, the over-flown scene was not limited to the area of interest, so, the orthophoto and DEM shown in Figs. 3 and 5, respectively include the neighbouring areas that were subsequently eliminated. The DEM obtained had a resolution of 0.03 m. Finally, the generated DEM has been converted to GRID format by interpolating the original points using the Kriging estimator.

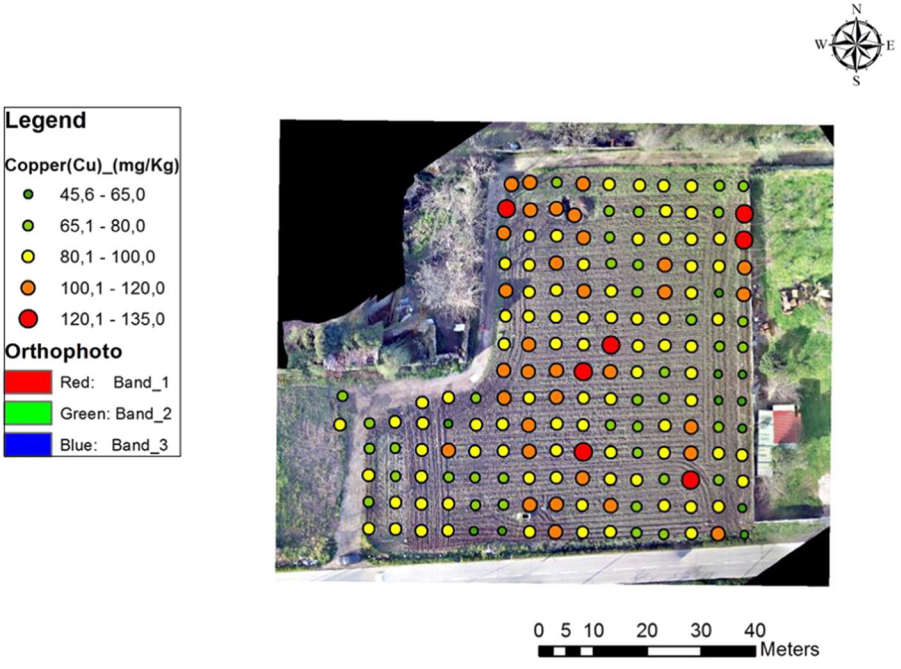

Fig. 3. Copper concentration classes (in mg/kg) over the obtained orthophoto map.

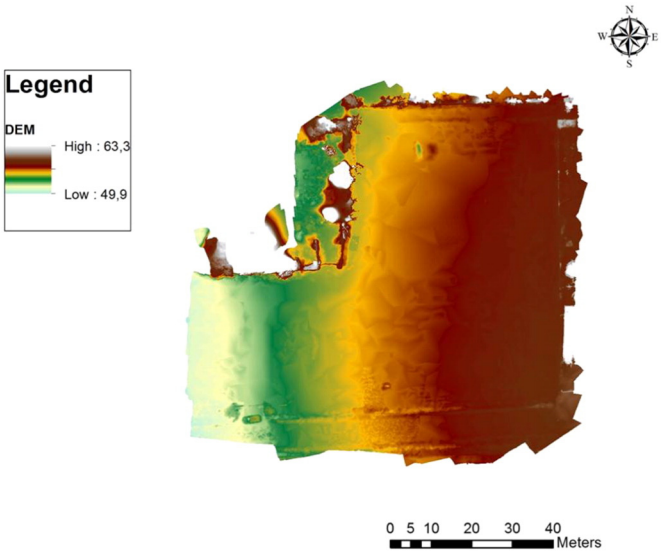

Fig. 5. Graph of the obtained Digital Elevation Model (DEM).

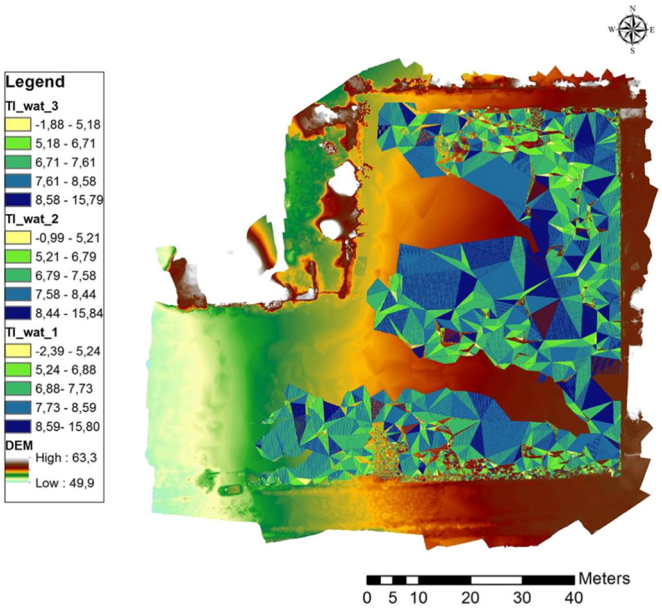

Fig. 7. Range of Topographic Index (TI) values.

4.3. Micro-rill and copper sedimentation points

The micro-rill network allowed for the generation of the flow direction, flow accumulation (relating to preferential paths of runoff water) and micro-basin rasters. In particular, the field has been divided in three micro basins illustrated by the upper red, the middle blue and the bottom green sections of the field as shown in Fig. 6. These sections covered an area of 1007.30 m^2, 1050.12 m^2 and 1001.54 m^2, respectively.

The average monthly rainfall amount has been found to be 78 mm, with a peak of 137.43 mm, in the period between 1977 and 1993. Also evapotranspiration was calculated in the same time range. The highest values of evapotranspiration have been observed during the summer months, with a monthly peak of 157.12 mm in July, while a minimum value of 27.23 mm was recorded in January. Average values of the effective monthly rainfall had a peak value of 77 mm in December and nulls in the warmer months from May to September. Therefore, the effective average annual rainfall has been evaluated to be 27 mm.

Finally, TI and CTI have been calculated in the three micro-basins of interest. As shown in Fig. 7, range of TI values was different in the three sections of the map. It varied between −2.39 and 15.80, −0.99 and 15.84, and −1.88 and 15.79 in the upper, middle and bottom sections, respectively. Also, CTI value given in Fig. 8 were significantly different in each of the three sections. Its values were between 2.47 and 18.21, 3.50 and 18.25 and 2.46 and 18.20 in the upper, middle and bottom zones, respectively.

In order to identify areas characterised by greater accumulation of copper, for each micro-basin, TI and CTI were processed through simple kriging interpolator and compared with the actual mapping of the

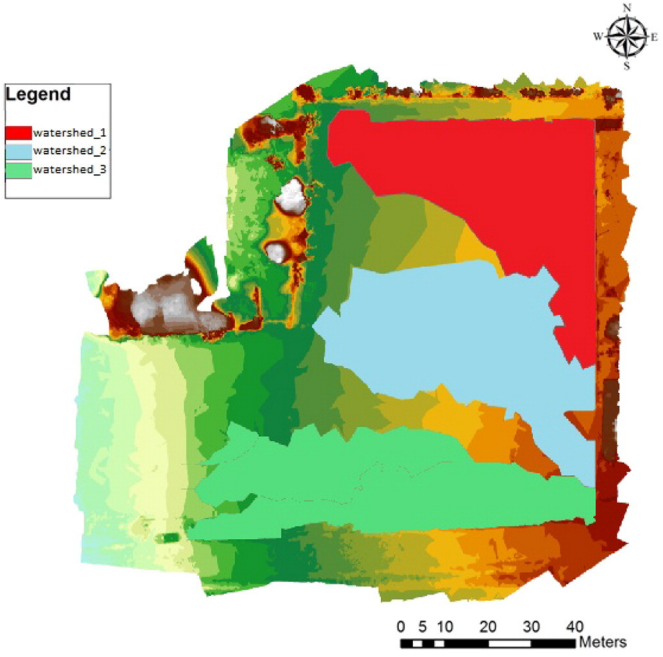

Fig. 6. Micro-basins in the study area over the obtained DEM graph. (For interpretation of the references to color in this figure legend, the reader is referred to the web version of this article.)

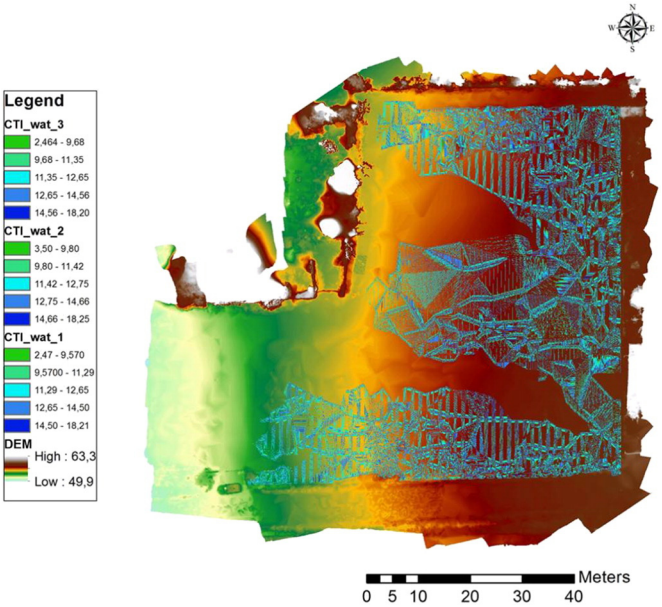

Fig. 8. Range of Clima-Topographic Index (CTI) values.

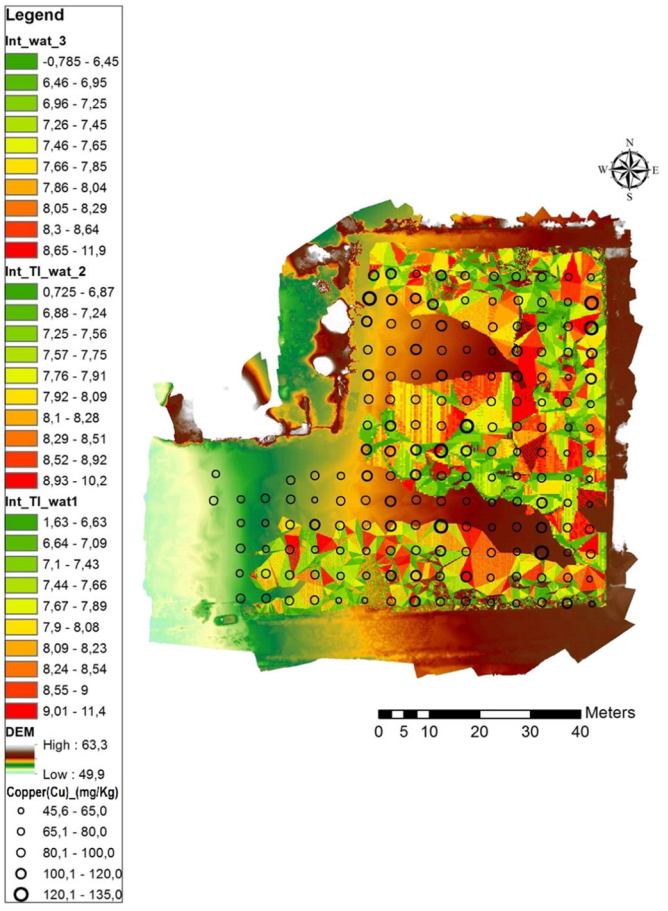

Fig. 9. Range of Interpolated Topographic Index for the three different watersheds.

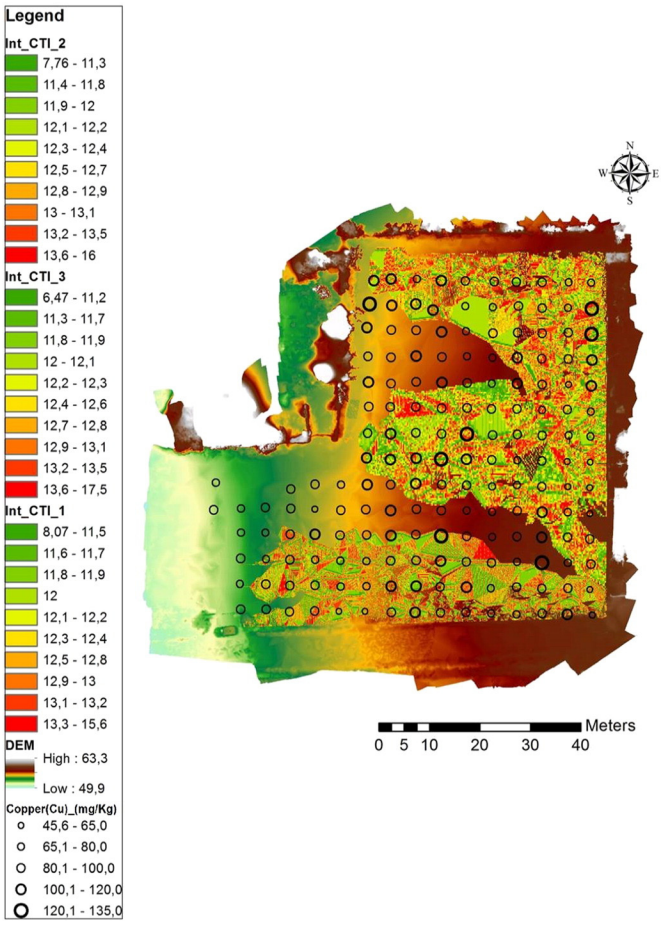

Fig. 10. Range of interpolated Clima Topographic Index for the three different watersheds.

copper on the soil surface (Figs. 9, 10). As shown in Fig. 9, ranges of values interpolated TI were found to be different in the three sections of the map. It varied between −1.63 and 11.36, 0.72 and 10.22, and −0.75 and 11.94 in the upper, middle and bottom sections, respectively. Also, CTI values were significantly different in each section (Fig. 10). Its values were between 8.06 and 15.55, 6.47 and 17.50 and 7.75 and 15.98 in the upper, middle and bottom zones, respectively.

In order to verify the relationship between the copper concentration and TI (or CTI), a "Boolean And" Operation was applied. Fig. 11 shows the results of the Boolean Operation between copper concentration, interpolated with indicator Kriging, and Topographic Index. This procedure points out five areas in which the maximum values of both raster coincide.

Fig. 12 shows the results of the Boolean Operation between the copper concentration, interpolated with indicator Kriging, and the Clima-Topographic Index. This method allows the identification of four points in which the maximum values of both rasters coincide.

5. Discussion

The use of photos taken using cameras mounted on drones and processed using a fifth generation software for photogrammetry introduces many benefits. The flight altitude of drones is lower than traditional airborne platform quotas; thus, allowing for acquisition of high resolution photos. In addition, the time required for data acquisition and the operational costs are drastically decreased (Nex and Remondino, 2014). The hexacopter flight was performed at a height of 25 m above ground surface at a travel speed of 4 m s^{-1}, unthinkable for a plane. For this reason, the accuracy of the DEM obtained was 0.03 m, making it suitable for studies of the micro-rill processes. Moreover, the data acquisition

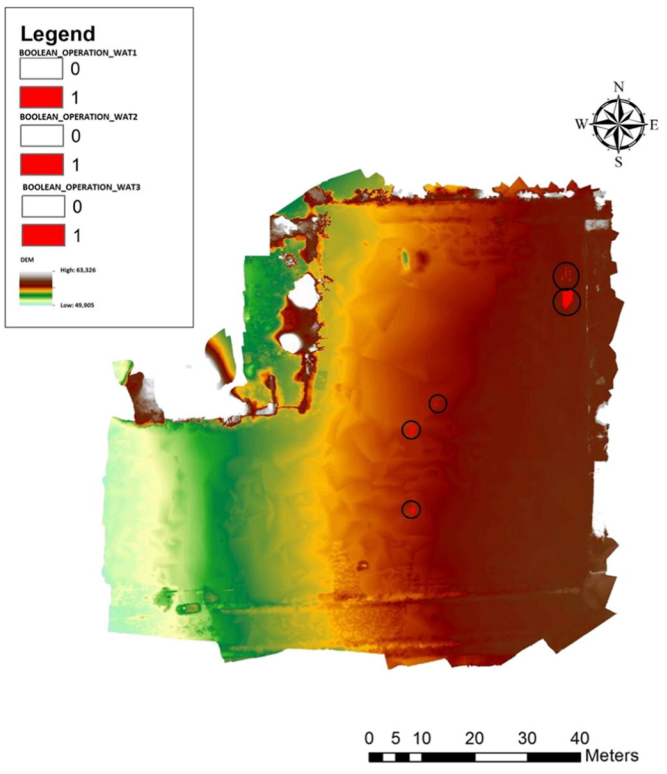

Fig. 11. Boolean And Operation between TI and interpolated copper concentration map.

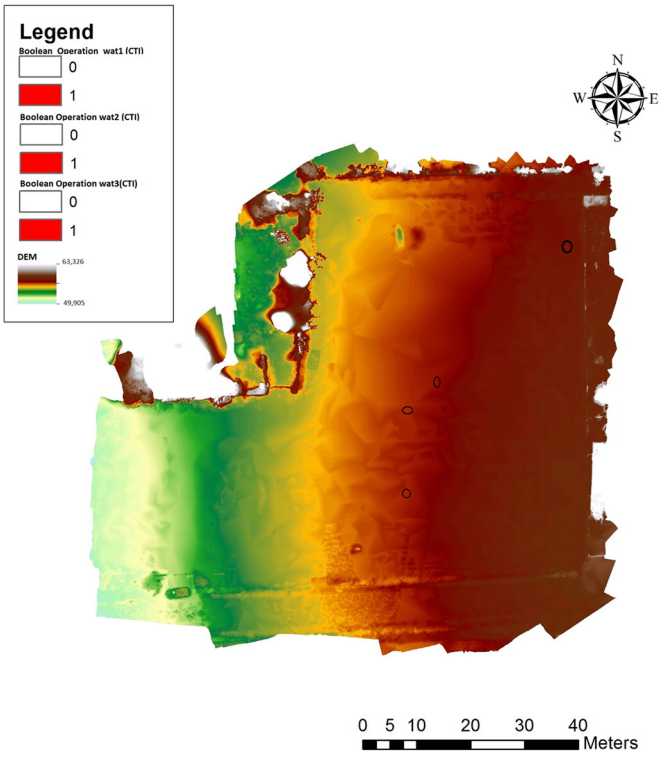

Fig. 12. Boolean And Operation between interpolated copper concentration and CTI.

times were relatively short. Data acquisition from the entire field was accomplished by a combination of three missions consisting of the first two, each characterized by 16 waypoints over a period of 12 min and the third, arranged over 12 waypoints and lasting 8 min. Consequently, the cost of all operation was relatively low. The processing of the captured frames with the fifth generation software allowed to significantly reduce the time of analysis as observed by Pierrot-Deseilligny et al. (2011). The DEM was obtained through the automatic restitution of the 84 frames in parallel.

The DEM obtained was used to determine micro-rill network in the study plot, which allowed for identification of three micro-basins. Results of copper mapping showed that 4.1% of the samples had concentration of copper above the legal limit of 120 mg kg^{-1} (T.U. Ambientale 471/99), and that about 17.6% of the samples were characterized by copper quantity close to the legal limit (100–120 mg kg^{-1}). The lower, the middle and the upper micro-basins are comprised by 28.6%, 28.6% and 42.8% of the hotspots with concentration of copper exceeding the legal limit, respectively.

On these basins, TI and CTI were then calculated. The TI values ranged between −2.39 and 15.80, −0.99 and 15.84 and −1.88 and 15.79 in the upper, middle and bottom of the study plot. The differences in values observed were attributed to the various slopes of the basins and to the diverse drainage areas. In addition, it was observed that for a given area, TI value increased with the reduction of the slope. From the physical point of view, this means that the possibility of accumulation of water on land with steeper slope is lower than on flat land. This therefore gives an important indication of the variability of soil moisture; that is, increasing TI value is related to higher saturation of the soil. It is assumed that these zones correspond to copper sedimentation points.

However, the CTI value varied between 2.47 and 18.21, 3.50 and 18.25 and 2.46 and 18.20 in the upper, middle and bottom portions of the plot, respectively. Also in this case, the differences in values are due to the varying slopes of the basins and the diversity of drainage areas. The CTI is a more robust index, because it correlates the topographical features of the field and climatic events. The larger the drainage area, the more is the intensive effective rain, and the lower the slope is, the higher is the CTI value. Therefore, for a given area and rainfall event, CTI will depend in particular on the slope. So, just like in the previous case, the greatest accumulation of water appears in the flat areas. For this reason, the saturation degree of flat areas is higher. It is assumed that these zones correspond to the copper sedimentation points. Moreover, the replacement of the local slope with the downhill slope allowed for consideration of both the upslope component and the downslope factor.

From the foregoing it can be observed that the two indices have different saturation values because of the replacement of the slope and of the implication of the effective rainfall in the calculation of the CTI. These characteristics improve the results from the technical point of view, as well as from the conceptual point of view, as also observed by Gascuel-Odoux et al. (1998). In fact, the local slope substitution with the downhill element led us to take into account both downslope and upslope, while the implication of the effective rainfall led us to take into account the weather conditions. In addition, CTI showed higher potential to determine the location and general area extent of wetlands in a reliable manner, even without calibration. However this potential was observed to decline when the soils were characterized by a high heterogeneous permeability (Merot et al., 2003). For these reasons, it seems likely that the CTI would be more suited for the identification of sedimentation points for heavy metals.

The interpolation of TI and CTI allows to identify areas in which is expected a higher accumulation of copper (red zones) and those in which the concentration is lower (orange, yellow, green). Comparing the two maps, it is clear that the interpolated TI is possible to pinpoint areas of accumulation more easily, while the interpolated CTI indentifies accumulation points more precisely. This study shows that all points with a value equal to or higher than the legal limit and the majority of those with a value close to the legal limit are contained in the micro-basins identified, particularly in areas with a highest value of TI and CTI. Therefore, the red areas correspond to the zones in which the copper value is definitely higher than the neighbouring ones, and therefore, probably, can be found a concentration value equals or exceeds the normative value. This result is also confirmed by the maps shown in Figs. 11 and 12. In fact, the Boolean And Operation between copper concentration, interpolated with indicator Kriging, and TI indentifies five areas. For these ones, highest values of TI and copper concentration coincide. In this way, they are not identified the areas of the two points at the edge of the upper and lower basins. The Boolean And Operation between copper concentration, interpolated with indicator Kriging, and CTI, locates four points. Here, the highest values of the two rasters coincide. It cannot identify the points at the edge of the upper and lower basins and only one point within of the upper watershed.

The organization of the sampling companies has been made according to the results of this approach of such information. Consequently, it is convenient to concentrate the sampling only in the micro-basins identified and, in particular, in the “red zones”. Following the analysis of these samples, you must assess whether or not to continue the sampling procedure. In fact, if all the red areas show values lower than the legal limit, the sampling can be stopped, otherwise it might be appropriate to sample areas corresponding to values of TI and CTI gradually lower.

6. Conclusion

In this paper, a novel approach that combines photogrammetric technique with hydrological models was tested, (Merot et al., 2003; Gascuel-Odoux et al., 1998) in the prediction of accumulation sites of trace elements, that can be mobilised adhering to organic matter. In this case, the approach was used to predict copper accumulation sites in an experimental field, and it turned out to be very promising. Specifically it considerably reduces the soil sampling requirements, making it necessary to take samples only in the areas where copper sedimentation points are expected. Geostatistcs was confirmed as the method to be

used to spatialize hydrological models (Castrignanò et al., 2011). Copper concentration observed in the field test does not exceed the range values reported by Albanese et al. (2007).

In conclusion the method proposed for the detection of critical sampling points for the characterization of polluted soils, seems to be robust, rapid and most economic compared to the traditional techniques for the characterization of the soil with the ordinary mesh of 5 × 5 m. Therefore, it appears that it could play a key role in future development of environmental monitoring techniques. For example, it could be used as a model for the development of similar methods for detecting other heavy metals or the parasites that live in the wetlands. Moreover, another possible field of investigation deals with management of fertilizing activities for the prediction of nutrient in the soil.

Acknowledgements

This study was financed by the Life Ecoremed Project (LIFE11/ENV/IT/275) and by the ENERBIOCHEM Project (PON 01_01966). The soil analysis of copper was carried on and kindly provided by Prof. Amoresano of the Mass Spectrometry Laboratory of University of Naples "Federico II"

References

Albanese, S., Cicchella, D., 2012. Legacy problems in urban geochemistry. Elements 8, 423–428.
Albanese, S., De Vivo, B., Lima, A., Cicchella, D., 2007. Geochemical background and baseline values of toxic elements in stream sediments of Campania Region (Italy). J. Geochem. Explor. 93 (1), 21–34.
Allen, R.G., Pereira, L.S., Raes, D., Smith, M., 1998. Crop evapotranspiration – Guidelines for computing crop water requirements. FAO Irrigation and Drainage Paper, FAO, Rome p. 56.
Beaujouan, V., Durand, P., Ruiz, L., 2001. Modelling the effect of the spatial distribution of agricultural practices on nitrogen fluxes in rural catchments. Ecol. Model. 137, 93–105.
Bertuzzi, P., Caussignac, J.M., Stengel, P., Morel, G., Lorendeau, J.Y., Pelloux, G., 1990. An automated, noncontact laser profile meter for measuring soil roughness in situ. Soil Sci. 149 (3), 169–178.
Beven, K., 1986. Runoff production and flood frequency in catchments of order n: an alternative approach. *Scale problem in hydrology*. Water Sci. Technol. Libr. 6, 107–131.
Beven, K.J., Kirkby, M.J., 1979. A physically based, variable contributing area model to basin hydrology. Hydrol. Sci. Bull. 24, 43–69.
Beven, K.J., Wood, E.F., Sivapalan, M., 1988. On hydrological heterogeneity—catchment morphology and catchment response. J. Hydrol. 100 (1), 353–375.
Buzzi, J., Riaza, A., García Meléndez, E., Carrère, V., Holzwarth, S., 2014. Monitoring of river contamination derived from acid mine drainage using airborne imaging spectroscopy (HyMap DATA, SOUTH-WEST SPAIN). River Res. Appl. http://dx.doi.org/10.002/rra.2849.
Capolupo, A., Pindozzi, S., Okello, C., Boccia, L., 2014. Indirect field technology for detecting areas object of illegal spills harmful to human health: application of drones, photogrammetry and hydrological models. Geospat. Health 8 (3), 699–707.
Castrignanò, A., Stelluti, M., 1997. Metodi di studio della variabilità spaziale e delle proprietà fisiche del suolo. Riv. Di Agron 31 (2), 361–374.
Castrignanò, A., Goovaerts, P., Lulli, L., Bragato, G., 2000. A geostatistical approach to estimate probability of occurrence of *Tuber melanosporum* in relation to some soil properties. Geoderma 98 (3), 95–113.
Castrignanò, A., Lopez, R., Stelluti, M., 2011. Introduction to Spatial Data Processing. CRA.
Chirico, G.B., Grayson, R.B., Western, A.W., 2003. On the computation of the quasi-dynamic wetness index with multiple-flow-direction algorithms. Water Resour. Res. 39 (5).
Chirico, G.B., Western, A.W., Grayson, R.B., Blöschl, G., 2005. On the definition of the flow width for calculating specific catchment area patterns from gridded elevation data. Hydrol. Process. 19 (13), 2539–2556.
Cicchella, D., De Vivo, B., Lima, A., 2005. Background and baseline concentration values of elements harmful to human health in the volcanic soils of the metropolitan and provincial areas of Napoli (Italy). Geochem. Explor. Environ. Anal. 5 (1), 29–40.
De Vivo, B., Torok, K., Ayuso, R.A., Lima, A., Lirer, L., 1995. Fluid inclusion evidence for magmatic silicate/saline/CO_2 immicibility and geochemistry of alkaline xenoliths from Ventotene Island (Italy). Geochim. Cosmochim. Acta 59, 2941–2953.
Famiglietti, J.S., Wood, E.F., 1991. Evapotranspiration and runoff from large land areas: land surface hydrology for atmospheric general circulation models. Land Surface—Atmosphere Interactions for Climate Modeling. Springer, Netherlands, pp. 179–204.
Filippelli, G., Morrison, M., Cicchela, D., 2012. Urban geochemistry and human health. Elements 8, 439–444.
Gascuel-Odoux, C., Merot, P., Crave, A., Gineste, P., Taha, A., Zhang, Z., 1998. Les zones contributives de fond de vallée: localisation, structure et fonctionnement hydrodynamique. Agriculture intensive et qualité des eaux. Coll. Sciences Update, éd. INRA, p. 129-14.
Goovaerts, P., 1987. Geostatistics for Natural Resources Evaluation. Oxford University Press, New York, p. 483.
Gruen, A., Beyer, H.A., 2001. System calibration through self calibration. Calibration and orientation of cameras in computer vision. In: Gruen, Huang (Eds.), Springer Series In, Information Sciences 34, pp. 163–194.
Hargreaves, G.L., Hargreaves, G.H., Riley, J.P., 1985. Agricultural benefits for Senegal River basin. J. Irrig. Drain. Eng. 111 (2), 113–124.
Holmgren, P., 1994. Topographic and geochemical influence on the forest site quality, with respect to *Pinus sylvestris* and *Picea abies* in Sweden. Scand. J. For. Res. 9 (1–4), 75–82.
Huang, C., White, I., Thwaite, E., Bendeli, A., 1988. A noncontact laser system for measuring soil surface topography. Soil Sci. Soc. Am. J. 52, 350–355.
Infascelli, R., Faugno, S., Pindozzi, S., Boccia, L., Merot, P., 2013. Testing different topographic indexes to predict wetlands distribution. Procedia Environ. Sci. 19, 733–746.
Journel, A.G., 1983. Nonparametric estimation of spatial distributions. J. Int. Assoc. Math. Geol. 15 (3), 445–468.
Journel, A.G., Huijbregts, C.J., 1978. Mining Geostatistics. Academic Press, New York, NY, p. 600.
Kabata-Pendians, A., Pendias, H., 2001. Trace Elements in Soils. 3th ed. CRC Press, Boca Raton, London, New York, p. 413.
Khorashahi, J., Byler, R., Dillaha, T., 1987. An opto-electronic soil profile meter. Comp. Electron. Agric. 2, 145–1550.
Lagacherie, P., McBratney, A., Voltz, M., 2006. Digital Soil Mapping: An Introductory Perspective vol. 31. Elsevier.
Lima, A., Ghiaccio, I., Cicchella, D., Albanese, S., Bove, M.A., Grezzi, G., Ayuso, A.R., De Vivo, B., 2012. Atlante geochimico ambientale del SIN (Sito di Interesse Nazionale) litorale Domizio Flegreo e Agro Aversano. Aracne Editrice, Roma, Italy 9788854851481, p. 254.
Merot, P., Squividant, H., Aurousseau, P., Hefting, M., Burt, T., Maitre, V., Kruk, M., Butturini, A., Thenail, C., Viaud, V., 2003. Testing a climato-topographic index for predicting wetlands distribution along an European climate gradient. Ecol. Model. 63, 51–71.
Montreuil, O., 2011. Relation entre l'ordre des bassins versants, l'organisation spatiale et le fonctionnement hydrologique et hydrochimique des zones humides riveraines. Géosciences Rennes. Mémoires du CAREN1761-2810 vol. 1 (n. 28).
Moore, I.D., Norton, T.W., Williams, J.E., 1993. Modelling environmental heterogeneity in forested landscapes. J. Hydrol. 150 (2), 717–747.
Muscutt, A.D., Harris, G.L., Bailey, S.W., Davies, D.B., 1993. Buffer zones to improve water-quality — a review of their potential use in UK agriculture. Agric. Ecosyst. Environ. 45 (1–2), 59–77.
Nex, F., Remondino, F., 2014. UAV for 3D mapping applications: a review. Appl. Geomat. 6 (1), 1–15. http://dx.doi.org/10.1007/S12518-013-0120-x.
O' Callaghan, J.F., Mark, D.M., 1984. The extraction of drainage networks from digial elevation data. Comp. Vision Graph. Image Process. 28, 323–344.
O'loughlin, E.M., 1981. Saturation regions in catchments and their relations to soil and topographic properties. J. Hydrol. 53 (3), 229–246.
Oosterbaan, R.J., Nijland, H.J., 1994. Determining the saturated hydraulic conductivity. In: Ritzema, H.P. (Ed.), Drainage Principles and Applications. International Institute for Land Reclamation and Improvement (ILRI) Publication 16, Wageningen, The Netherlands, pp. 435–476.
Pierrot-Deseilligny, M., De Luca, L., Remondino, F., 2011. Automated image-based procedures for accurate artifacts 3D modeling and orthoimage generation. Geoinform.s FCE CTU J. 6, 291–299 (Prague, Czech Republic).
Pindozzi, S., Faugno, S., Okello, C., Boccia, L., 2012. Experimental evaluation of manure evaporation in the paddock for a management algorithm development. Proceedings of International Conference of Agricultural Conference, pp. 8–12.
Pindozzi, S., Faugno, S., Okello, C., Boccia, L., 2013. Measurement and prediction of buffalo manure evaporation in the farmyard to improve farm management. Biosyst. Eng. 115 (2), 117–124.
Rieke-Zapp, D., Wegmann, H., Santel, F., Nearing, M.A., 2001. Digital photogrammetry for measuring soil surface roughness. Proceedings of the year 2001 Annual Conference of the American Society for Photogrammetry & Remote Sensing ASPRS, pp. 23–27 (April).
Robson, A., Beven, K., Neal, C., 1992. Towards identifying sources of subsurface flow: a comparison of components identified by a physically based runoff model and those determined by chemical mixing techniques. Hydrol. Process. 6 (2), 199–214.
Romenkens, M., Singaraya, S., Gantzer, C., 1986. An automated noncontact surface profile meter. Soil Tillage Res. 6, 193–202.
Sivapalan, M., Wood, E.F., 1987. A multidimensional model of nonstationary space-time rainfall at the catchment scale. Water Resour. Res. 23 (7), 1289–1299.
Sivapalan, M., Wood, E.F., Beven, K.J., 1990. On hydrologic similarity: 3. A dimensionless flood frequency model using a generalized geomorphologic unit hydrograph and partial area runoff generation. Water Resour. Res. 26 (1), 43–58.
Sörensen, R., Zinko, U., Seibert, J., 2006. On the calculation of the topographic wetness index: evaluation of different methods based on field observations. Hydrol. Earth Syst. Sci. Discuss. 10 (1), 101–112.
Stevenson, F.J., Ficht, A., 1981. Reaction with organic matter. In: Lonergan, F.J., Robson, A.D., Graham, R.D. (Eds.), Copper in Soils and Plants. Academic Press, New York, pp. 69–95.
Swaine, D.J., 1962. The trace-element content of fertilizers. Soil Sci. 94 (2), 134.
Tavares, M.T., Sousa, A.J., Abreu, M.M., 2008. Ordinary kriging and indicator kriging in the cartography of trace elements contamination in São Domingos mining site (Alentejo, Portugal). J. Geochem. Explor. 98 (1), 43–56.
Triggs, B., McLauchlan, P.F., Hartley, R.I., Fitzgibbon, A.W., 2000. Bundle adjustment—a modern synthesis. Vision Algorithms: Theory and Practice. Springer, Berlin Heidelberg, pp. 298–372.
Vito, M., Merola, G., Giordano, A., Ragone, G., 2009. Relazione sullo stato dell'ambiente in Campania. pp. 327–349 (Avaible at http://www.arpacampania.it/documents/30626/52179/7_RSA+2009.pdf, accessed on June 2013).
West, B.J., Shlesinger, M., 1990. The noise in natural phenomena. Am. Sci. 40–45.
White, J.D., Running, S.W., 1994. Testing scale dependent assumptions in regional ecosystem simulations. J. Veg. Sci. 5 (5), 687–702.
Wolock, D.M., McCabe, G.J., 1995. Comparison of single and multiple flow direction algorithms for computing topographic parameters in TOPMODEL. Water Resour. Res. 31, 1315–1324.